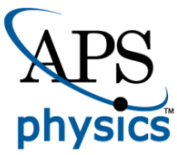



# Observation of Drastic Electronic-Structure Change in a One-Dimensional Moiré Superlattice

Sihan Zhao, Pilkyung Moon, Yuhei Miyauchi, Taishi Nishihara, Kazunari Matsuda, Mikito Koshino, and Ryo Kitaura

Phys. Rev. Lett. **124**, 106101 — Published 9 March 2020

DOI: 10.1103/PhysRevLett.124.106101

# Observation of drastic electronic structure change in one-dimensional moiré crystals

Sihan Zhao[1]*, Pilkyung Moon[2], Yuhei Miyauchi[3], Taishi Nishihara[3], Kazunari Matsuda[3], Mikito Koshino[4], and Ryo Kitaura[5]*.

[1]Department of Physics, University of California at Berkeley, Berkeley, California 94720, USA

[2]New York University Shanghai, Pudong, Shanghai 200120, China

[3]Institute of Advanced Energy, Kyoto University, Uji, Kyoto 611-0011, Japan

[4]Department of Physics, Osaka University, Toyonaka 560-0043, Japan

[5]Department of Chemistry & Institute for Advanced Research, Nagoya University, Nagoya 464-8602, Japan

*To whom correspondence should be addressed.
sihanzhao88@berkeley.edu, r.kitaura@nagoya-u.jp

**Abstract:** We report the first experimental observation of strong coupling effect in one-dimensional moiré crystals. We study one-dimensional double-wall carbon nanotubes (DWCNTs) in which van der Waals-coupled two single nanotubes form one-dimensional moiré superlattice. We experimentally combine Rayleigh scattering spectroscopy and electron beam diffraction on the same individual DWCNTs to probe the optical transitions of structure-identified DWCNTs in the visible spectral range. Among more than 30 structure-identified DWCNTs examined, we experimentally observed and identified a drastic change of optical transition spectrum in DWCNT with chirality (12,11)@(17,16). The origin of the marked change is attributed to the strong intertube coupling effect in a moiré superlattice formed by two nearly-armchair nanotubes. Our numerical simulation is consistent to these experimental findings.

Engineering the electronic band structures through the formation of moiré superlattice has enabled the discoveries of exotic physics in two-dimensional (2D) van der Waals-coupled heterostructures [1-16]. Such band structure engineering through the formation of moiré superlattice can lead to significant alternation of the electronic properties in the coupled heterostructures. One of the impressive examples is to control the mutual angle between two graphene monolayers to form the twisted bilayer graphene [5-9]. The flat band caused by a moiré superlattice structure gives rise to Mott insulating state and superconducting state at certain twisted "magic" angles, which, on the other hand, do not exist in the pristine monolayers. Moiré superlattice formed between 2D semiconductors also leads to the observation of "moiré excitons" which is a direct consequence of drastic band structure change caused by moiré superlattice [11-16].

While there has been a rapid progress on understanding the moiré physics in 2D heterostructures, experimental studies on moiré superlattice in one-dimensional (1D) systems are still limited, and no clear evidence on strong electronic structure modification has been made and explained in structure-identified 1D moiré superlattices [17-20]. Double-wall carbon nanotubes (DWCNTs), which correspond to a "rolled up" version of twisted bilayer graphene, naturally provide an ideal platform to experimentally probe the moiré physics in 1D. Theoretically, it was assumed that the electronic band structures of realistic DWCNTs are close to those of the individual constituent two single nanotubes, and the effect of the intertube coupling is perturbative [21-24]. Most of previous experimental observations on intertube coupling effect are well-explained within the weakly perturbative regime [25-28]. However, a recent theoretical study predicted that there are special cases where the moiré superlattice potential causes strong coupling between two single nanotubes and can result in completely different band structures [29].

Here we show the experimental evidence of the strong coupling effect in 1D moiré crystals where the moiré superlattice potential significantly alters the electronic band structures in DWCNTs. The lattice structure of each constituent nanotube, consequently the moiré superlattice formed in DWCNT, is determined by electron beam diffraction and the corresponding electronic transitions of the same DWCNT are probed by Rayleigh scattering spectroscopy in the visible spectral range. Though rarely observed in all examined DWCNTs, one specific DWCNTs show drastic changes in Rayleigh scattering spectra, which is assigned to be a direct consequence of the strong coupling between two constituent single nanotubes. The calculated band structure and optical absorption spectra with intertube coupling within the effective continuum model support our experimental interpretation. Our experimental observation of strong coupling effect in 1D DWCNT moiré crystals can open up new opportunities to explore the rich moiré physics in 1D systems.

To investigate the intrinsic moiré physics in DWCNTs, we directly grew suspended DWCNTs with high-quality across an open slit (~ 30 μm in width) by chemical vapor deposition. We studied the individual DWCNTs that are isolated from other nanotubes. The structure (i.e. the chirality) of each constituent single nanotube comprising a DWCNT was determined by the nano-beam electron diffraction with a transmission electron microscope operated at 80 keV (JEOL-2100F). Electronic transitions of the DWCNTs with known chiralities are probed by Rayleigh scattering spectroscopy. In brief, a broadband light from a supercontinuum laser source (1.2 eV – 2.75 eV) was focused on the central part of the suspended DWCNT samples and the laser light was polarized along the nanotube axis to probe optical transitions within the same 1D subbands. The light scattered by the nanotube was collected and directed to a CCD camera and a spectrometer. The Rayleigh scattering spectra were obtained by normalizing the measured scattered light with incident laser intensity.

Most of structure-identified DWCNTs were found in a weak-coupling regime [26,28]. Two representative Rayleigh spectra for individual DWCNTs with weak-coupling are shown in **Figs. 1a** and **1b**. The chiralities of the two DWCNTs are determined as (15,13)@(21,17) and (23,4)@(22,18) by the nano-beam electron diffraction, respectively. (15,13) and (21,17) in (15,13)@(21,17) correspond to the chirality of inner nanotube and outer nanotube, respectively, and we keep this notation for indexing DWCNTs throughout the paper. As clearly seen in the spectra, multiple pronounced optical resonances are observed

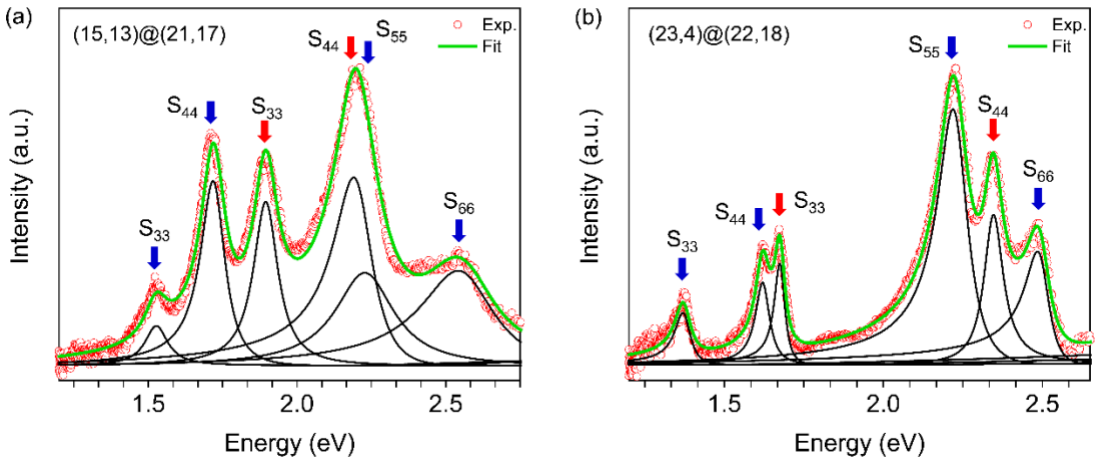


**Figure 1.** Rayleigh scattering spectra of two typical structure-identified DWCNTs with weak-coupling. **(a)** Spectrum for DWCNT (15,13)@(21,17). **(b)** Spectrum for DWCNT (23,4)@(23,18). In both (a) and (b), red and blue arrows mark the optical transitions for inner and outer nanotubes, respectively. The experimental data are presented by red open circles. Each fitted optical transition is presented with black curve and the overall fitted spectrum is shown by solid green line.

in both DWCNTs. Each optical resonance in the spectra arises from the dipole-allowed interband transitions within the same 1D subbands from inner and/or outer nanotubes. For example, in (15,13)@(21,17) shown in Fig. 1a, four peaks indicated by the blue arrows are assigned to the $S_{33}$, $S_{44}$, $S_{55}$, and $S_{66}$ optical transitions from the outer nanotube (21,17), and those indicated by the red arrow are the $S_{33}$ and $S_{44}$ optical transition from the inner nanotube (15,13).

To investigate intertube interaction in detail, we precisely determine the resonant transition energies through peak deconvolution with fitting each of the resonances by the form of $I(\omega) \propto \omega^3|\chi(\omega)|^2$, where $\chi(\omega) \sim A_0 + [(\omega_0 - \omega) - i\gamma/2]^{-1}$. $I(\omega)$, $\chi(\omega)$, $\gamma$, and $A_0$ represent peak intensity, optical susceptibility, full width at half maximum (FWHM) associated with a resonance peaked at $\omega_0$, and non-resonant constant background that accounts for the asymmetric Rayleigh peak shape [30]. The fitted curve of each "Lorentzian-like" optical resonance is shown as the black line and the overall fitted spectrum is presented by the green line. The optical transition energies (i.e. $\omega_0$) for the two DWCNTs are summarized in **Supplemental Material Sec. 1** [31]. Comparing with the transition energies in isolated single nanotubes in air [32], all the optical resonances observed in DWCNTs with weak-coupling exhibit noticeable energy redshifts (some can show blue shifts) by few tens to two hundred meV.

While most of DWCNTs investigated are within the weak-coupling regime, where DWCNTs show almost identical electronic transitions to those of each individual constituent nanotube, we experimentally identified two DWCNTs whose electronic transitions are theoretically predicted to be very different from those of constituent single nanotubes due to a non-perturbative intertube coupling between the inner and outer nanotubes [29]. Theoretically, van der Waals coupling between inner and

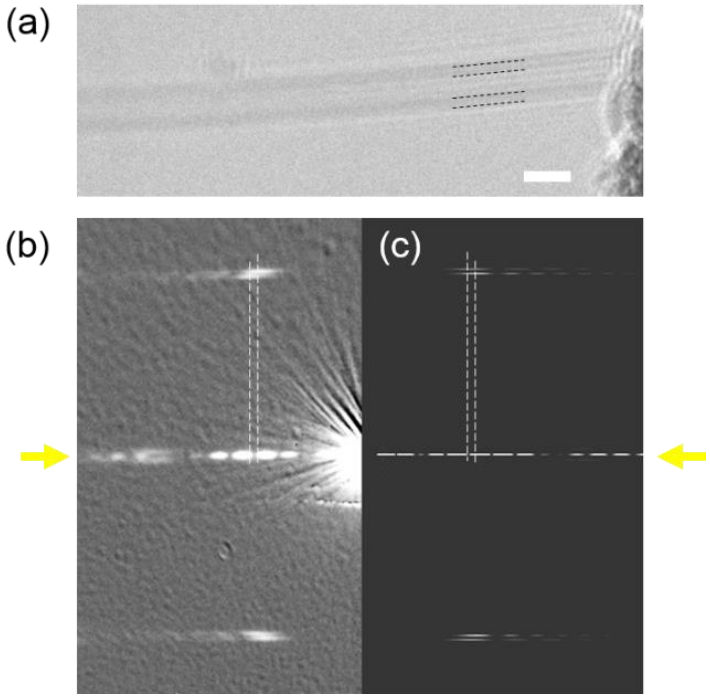


**Figure 2.** Structure characterization of a DWCNT (12,11)@(17,16) showing strong coupling effect. **(a)** TEM image of the DWCNT. Dashed lines indicate the walls of two constituent nanotubes. Scale bar is ~ 2 nm. **(b)** Experimental electron diffraction pattern. **(c)** Simulated electron diffraction pattern of DWCNT with chirality (12,11)@(17,16). Two yellow arrows indicate the position of equatorial line in diffraction pattern. The dashed lines are eye guidance to show one of the key identities between experiment and simulation.

outer nanotubes in DWCNT moiré superlattices is essentially characterized by the relative orientation of chiral vectors (chiralities) of inner and outer nanotubes, C and C'. Significant modification of the band structure takes place under two different conditions, which we call the strong-coupling case and the flat-band case. The former occurs when C and C' are nearly parallel to each other and at the same time the difference of two chiral vectors C' − C is parallel to the armchair direction. Then the moiré superlattice potential makes the resonant coupling between the states of constituent nanotubes, and this leads to drastic energy shift of the subband edges. The latter case occurs under the condition that C and C' are nearly parallel and C' − C is parallel to the zigzag direction. There a long period moiré interference potential turns the original single nanotube bands into a series of nearly flat bands. When C and C' meet either of these two conditions, the electronic structures of DWCNTs become drastically different from the simple sum of constituent single nanotubes [29].

It is easy to see that none of the two weak-coupled DWCNTs shown in Fig. 1 meets the conditions described above. In fact, there is a lot less chance to have a DWCNT meeting the strong coupling criteria. For example, the probability for DWCNTs to satisfy the former criterion is only ~ 0.6% (**Supplemental Material Sec. 2** [31]). Although we still expect some moderate change of electronic structures in DWCNTs near the criteria, the effects of coupling become weaker as the configuration of C and C' deviates from the criteria. Hereafter we will focus on a strong-coupling case, (12,11)@(17.16) DWCNT, which accurately matches the former criterion. Experimental data for (14,3)@(23,3) DWCNT which approximately matches the latter condition are shown in **Supplemental Material Sec. 3 and Sec. 4** [31].

**Figure 2a** displays a transmission electron microscopy (TEM) image of a DWCNT in strong coupling regime. Although the TEM image becomes blurred away from the slit edge due to the vibration arising from the suspended structure, it is clear that there are contrasts originating from both inner and outer nanotubes. Judging from the TEM image, this DWCNT comprises an outer nanotube with a diameter ~ 2.2 nm and an inner nanotube with a diameter ~ 1.5 nm with a reasonable intertube distance (~ 0.35 nm). To ambiguously determine the physical structure of each nanotube, electron beam diffraction is employed and an observed diffraction pattern is presented in **Fig. 2b**. Similar to single chiral nanotubes in general, the diffraction pattern of a DWCNT shows sets of mutually twisted hexagonal patterns, which arise from hexagonal lattice of graphitic layers. Prior to any analysis in detail [37], Fig. 2b shows that the two constituent nanotubes are both nearly armchair nanotubes. The equatorial line in the DWCNT diffraction pattern exhibits a "beating-like" oscillation in intensity, which is absent in diffraction patterns in single nanotubes. This unique intensity oscillation originates from the interference of electron waves scattered by two nanotubes in the radial direction. Because of the high sensitivity of the interference to diameter and/or chirality of each nanotube, the oscillation profile along the equatorial line serves as a decisive

feature for unambiguous determination of DWCNT chirality. The intensity profile of equatorial line cut in Fig. 2a is further shown in **Supplemental Material Sec. 5** [31]. Based on the analysis procedures reported in literature [38], the chirality for the inner nanotube is determined to be (12,11) and that for the outer nanotube is (17,16). The simulated diffraction pattern of DWCNT (12,11)@(17,16) is shown in **Fig. 2c** for comparison, which shows an excellent agreement with the observed diffraction pattern in experiment. We note that one of the key identities between the Fig. 2b and 2c is indicated by dashed lines where the relative position for features on and outside equatorial line sensitively depend on the detailed chirality of each constituent single nanotubes. We show in **Supplemental Material Sec. 6** [31] the simulated pattern of a DWCNT with chirality (12,11)@(16,15), where chirality of the outer nanotube is slightly different from that of the right chirality DWCNT, (12,11)@(17,16). The discrepancy between experimental result (Fig. 2b) and the simulated pattern of (12,11)@(16,15) is apparent. We systematically examined all the possible candidates with simulation and confirmed that only (12,11)@(17,16) matches the experimental result (**Supplemental Material Sec. 7** [31]).

The inner and outer nanotubes in (12,11)@(17,16) are nearly armchair nanotubes, which means that C and C' are nearly parallel to each other (~ 0.4 degree chiral angle difference). In addition, C' − C is (5,5) that is strictly along the armchair direction. (12,11)@(17,16) DWCNT is, therefore, a strong-coupled DWCNT, whose band structure can be strongly modified by 1D moiré superlattice [29]. The Rayleigh spectrum of the same DWCNT (12,11)@(17,16) within our experimental energy range 1.2 eV – 2.75 eV

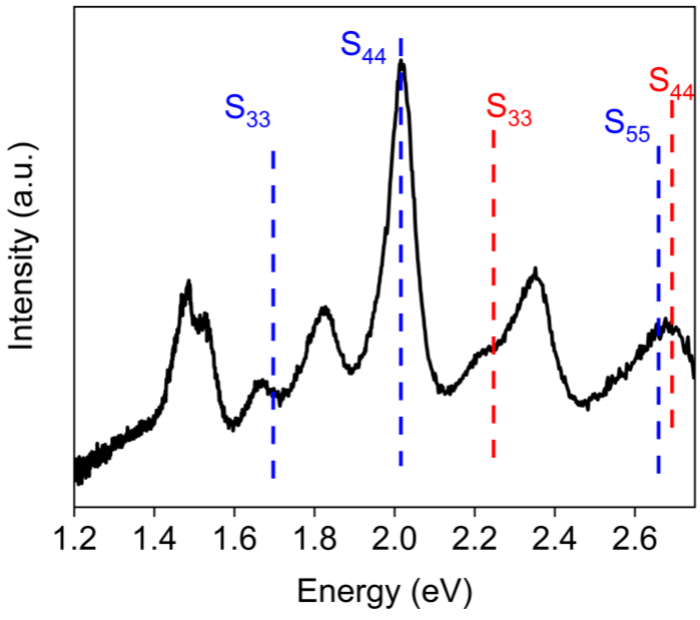


**Figure 3.** Rayleigh spectrum of DWCNT (12,11)@(17,16) showing strong coupling effect. Experimental data are shown in solid black. Dashed red and blue lines indicate the expected optical transition energies for pristine inner and outer nanotubes.

is presented in **Fig. 3**. Identical spectral profiles are obtained at different sample locations (**Supplemental Material Sec. 8** [31]). Markedly, we observed total eight well-defined optical resonances over the spectral range 1.2 – 2.75 eV; the weak peak at ~ 2.22 eV solely cannot be safely excluded to be a phonon sideband of the strong peak at ~ 2.02 eV [30,39-40]. On the other hand, within the same photon energy range, pristine (12,11) has two optical transitions $S_{33}$ at ~ 2.23 eV and $S_{44}$ at ~ 2.68 eV ($S_{22}$ at ~ 1.18 eV), and that pristine (17,16) has three optical transitions $S_{33}$ at ~ 1.69 eV, $S_{44}$ at ~ 2.03 eV and $S_{55}$ at ~ 2.66 eV ($S_{22}$ at ~ 0.90 eV) [32]. These referenced energy positions for inner and outer tubes are indicated by the red and blue dashed lines in Fig. 3. Unlike the weak-coupling cases (e.g. Fig. 1), where all optical transitions in DWCNTs correspond to interband transitions of individual constituent nanotubes, (12,11)@(17,16) shows optical resonances that cannot be assigned to those of pristine inner and outer nanotubes. As clearly seen, most of the observed transitions do not match those from each constituent nanotube with showing extra number of peaks expected from simple sum of two nanotube spectrum. These observations definitely manifest a drastic change of band structure in (12,11)@(17,16).

We attribute the observed drastic change of optical transition spectrum to the strong coupling effect arising from 1D moiré superlattice as the theory predicted [29]. By using the effective continuum model in the framework of a tight-binding (TB) approximation, we calculated the band structure and optical absorption spectrum for (12,11)@(17,16) (see details in **Supplemental Material Sec. 9** [31]). The calculated band structure of (12,11)@(17,16) without and with the intertube coupling are shown in **Figs. 4a** and **4b**, respectively. The band structure of pristine inner tube (12,11) and outer tube (17,16) are colored in red and blue in Fig. 4a, respectively. **Figure 4c** shows the calculated optical absorption spectrum of the coupled (12,11)@(17,16) (solid black) as well as the absorption spectra of the pristine inner and outer tubes (dashed red and blue) in the energy range 1.2 eV – 2.8 eV. The calculated absorption spectra for the pristine inner and outer nanotubes (dashed red and blue lines in Fig. 3) are consistent with experimental data in literature as well as our experimental results (dashed lines in Fig. 3) within a precision of ~ 100 meV [32] (**Supplemental Material Sec. 10** [31]).

In contrast to the weak-coupling cases shown in Fig. 1, the strong band hybridization caused by the intertube moiré superlattice potential of (12,11)@(17,16) drastically changes the electronic band structures (Figs. 4a and 4b) and selection rules from the simple sum of the constituent pristine nanotubes. Overall, our calculated absorption spectrum is qualitatively consistent with the experimental data in the same energy range. Figure 4c clearly shows the extra peaks observed in experiment but not identified in the pristine nanotubes. The number of transition peaks in the energy range 1.2 – 2.8 eV increases from 5 in the pristine nanotubes to 7, which is close to the actually observed number of 8. In fact, the peak around 2.4 eV in theoretical calculation is comprised of multiple peaks that are very close in energy (data

not shown), so they might be separated by many-body effects. Thus, the theoretical calculation supports the drastic difference between the observed spectrum and the spectrum of the constituent nanotubes in DWCNT at strong-coupling condition.

Before ending, we would like to briefly discuss and exclude other possibilities that can potentially lead to observation of very distinct spectrum. Structural inhomogeneity such as change of nanotube chirality, attachment of small nanotubes and/or impurities can cause very different optical response. In this study, the structure of DWCNT (12,11)@(17,16) is retained the same over the whole suspended region (~ 30 μm) where we confirmed the same structure from electron diffraction (**Supplemental Material Sec. 11** [31]). We also reassure that the Rayleigh signals observed in Fig. 3 do not include any other nearby nanotubes with a careful low-magnification TEM examination. DWCNT (12,11)@(17,16) also exhibit reasonably uniform Rayleigh optical response when tracing the laser beam along its axis (also see **Supplemental Material Sec. 8** [31]), with no sign of presence of large impurities. Transitions between different

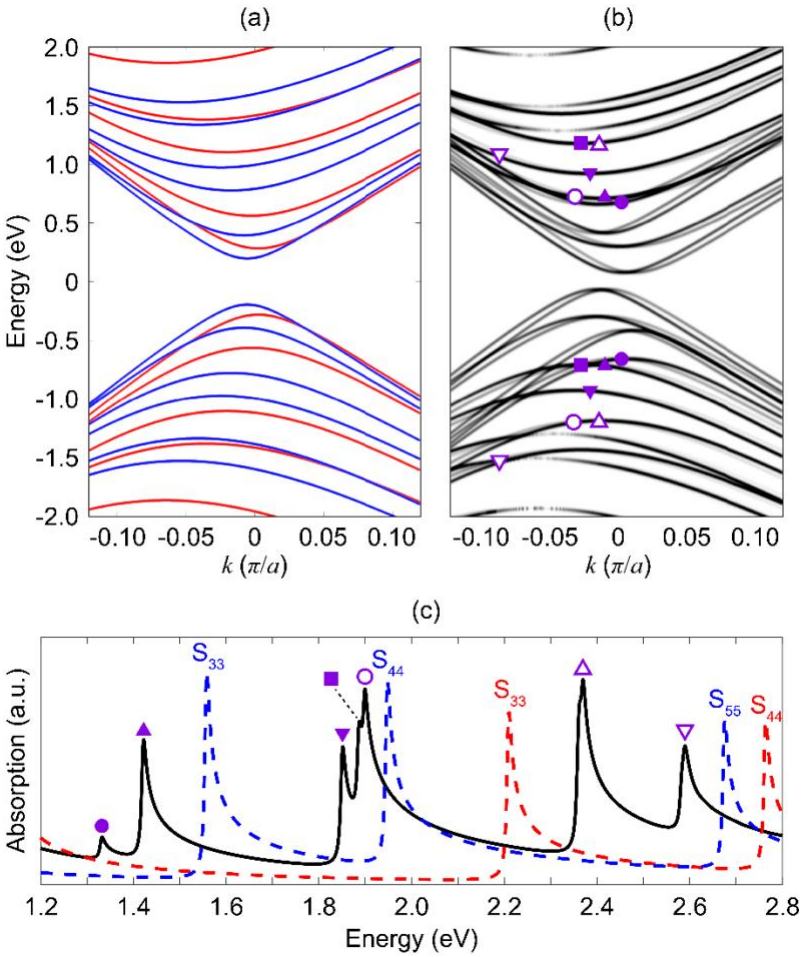


**Figure 4.** Theoretical calculation within tight-binding and effective continuum model. **(a)** Calculated band structure of two pristine nanotubes (12,11) and (17,16) in DWCNT without intertube coupling. **(b)** Calculated band structure of coupled DWCNT (12,11)@(17,16). (c) Calculated optical absorption spectra for pristine inner nanotube (dashed red), pristine outer nanotube (dashed blue) and the coupled DWCNT (solid black). Optical transitions from pristine inner and outer nanotubes are specified (e.g. $S_{33}$, $S_{44}$ etc.). Different transitions for the coupled DWCNT in (c) are denoted by different makers which originate from interband transitions as indicated with the same makers in the calculated band structure in (b). Note that the peak at ~ 2.4 eV (solid black) is comprised of multiple peaks that are very close in energy.

subbands (e.g. $S_{13}$, $S_{24}$ etc.) from each individual constituent nanotubes also cannot explain our experimental observation. Theses transitions are not allowed when laser polarization direction is parallel

to nanotube axis as in our experiment [41]. The optical response measured with cross-polarized laser beam is found negligibly small (**Supplemental Material Sec. 12** [31]). Emission from single defects also cannot explain the extra peaks since if exist, they would emit light with energy well below visible range (bandgap of outer nanotube lies in mid-IR).

In summary, we show the first experimental observation of strong coupling effect in structure-identified 1D moiré crystals. Through combining TEM-based chirality assignment and optical susceptibility measurements with Rayleigh scattering spectroscopy, we have successfully observed optical responses from a strong-coupled DWCNT, (12,11)@(17,16). In contrast to DWCNTs in the much more frequently observed weak-coupling regime, such as (15,13)@(21,17) and (23,4)@(22,18), the Rayleigh scattering spectrum of (12,11)@(17,16) cannot be understood based on simple sum of individual (12,11) and (17,16) nanotubes. Our numerical simulation shows that the moiré superlattice potential leads to significant alternation of the band structure of (12,11)@(17,16) and the corresponding optical spectra, which is consistent to our experimental observation and interpretation. This is the first definitive experimental observation of moiré superlattice effect in a structure-identified 1D system, which will lead to extended exploration of rich moiré physics in 1D such as strongly-correlated physics, moiré excitons and superconductivity.

**Acknowledgements:** We would like to thank Dr. SeokJae Yoo in the Department of Physics, UC Berkeley for the helpful discussion. This work was supported by JSPS KAKENHI Grant numbers JP16H06331, JP16H03825, JP16H00963, JP15K13283, JP25107002, and JST CREST Grant Number JPMJCR16F3.

**References:**


1. Dean, C. R. *et al.* Hofstadter's butterfly and the fractal quantum Hall effect in moiré superlattices. *Nature* **497,** 598–602 (2013).
2. Ponomarenko, L. A. *et al.* Cloning of Dirac fermions in graphene superlattices. *Nature* **497,** 594–597 (2013).
3. Hunt, B. *et al.* Massive Dirac Fermions and Hofstadter Butterfly in a van der Waals Heterostructure. Science **340,** 1427 (2013).
4. Geim, A. K. & Grigorieva, I. V. Van der Waals heterostructures. *Nature* **499,** 419–425 (2013).
5. Bistritzer, R. & MacDonald, A. H. Moiré bands in twisted double-layer graphene. PNAS **108,** 12233–12237 (2011).
6. Cao, Y. *et al.* Correlated insulator behaviour at half-filling in magic-angle graphene superlattices. Nature 556, 80–84 (2018).
7. Cao, Y., Fatemi, V., Fang, S., Watanabe, K., Taniguchi. T., Kaxiras E., Jarillo-Herrero, P. Unconventional superconductivity in magic-angle graphene superlattices. Nature **556,** 43–50 (2018).
8. Po, H. C., Zou, L., Vishwanath, A. & Senthil, T. Origin of Mott Insulating Behavior and Superconductivity in Twisted Bilayer Graphene. *Physical Review X* **8,** 31089 (2018).
9. Koshino, M. *et al.* Maximally Localized Wannier Orbitals and the Extended Hubbard Model for Twisted Bilayer Graphene. *Physical Review X* **8,** 31087 (2018).
10. Chen, G. *et al.* Evidence of a gate-tunable Mott insulator in a trilayer graphene moiré superlattice. *Nature Physics* **15,** 237–241 (2019).
11. Yu, H., Liu, G. Bin, Tang, J., Xu, X. & Yao, W. Moiré excitons: From programmable quantum emitter arrays to spin-orbit–coupled artificial lattices. *Science Advances* **3,** e1701696 (2017).
12. Wu, F., Lovorn, T. & Macdonald, A. H. Topological Exciton Bands in Moiré Heterojunctions. *Physical Review Letters* **118,** 1–6 (2017).
13. Tran, K. *et al.* Evidence for moiré excitons in van der Waals heterostructures. *Nature* **567,** 71–75 (2019).
14. Seyler, K. L. *et al.* Signatures of moiré-trapped valley excitons in MoSe2 /WSe2 heterobilayers. *Nature* **567,** 66–70 (2019).
15. Jin, C. *et al.* Observation of moiré excitons in WSe2/WS2 heterostructure superlattices. *Nature* **567,** 76–80 (2019).
16. Alexeev, E. M. *et al.* Resonantly hybridized excitons in moiré superlattices in van der Waals heterostructures. *Nature* **567,** 81–86 (2019).
17. Sanvito, S., Kwon, Y. K., Tománek, D. & Lambert, C. J. Fractional Quantum Conductance in Carbon Nanotubes. *Physical Review Letters* **84,** 1974–1977 (2000).
18. Kociak, M. *et al.* Linking Chiral Indices and Transport Properties of Double-Walled Carbon Nanotubes. *Physical Review Letters* **89,** 155501 (2002).
19. Tison, Y., Giusca, C. E., Stolojan, V., Hayashi, Y. & Silva, S. R. P. The inner shell influence on the electronic structure of double-walled carbon nanotubes. *Advanced Materials* **20,** 189–194 (2008).
20. Bonnet, R. *et al.* Charge transport through one-dimensional Moiré crystals. *Scientific Reports* **6,** 1–7 (2016).
21. Kwon, Y. K., Saito, S., Tománek, D. Effect of intertube coupling on the electronic structure of carbon nanotube ropes. *Physical Review B - Condensed Matter and Materials Physics* **58,** R13314–R13317 (1998).

22. Lambin, Ph., Meunier, V., Rubio, A. Electronic structure of polychiral carbon nanotubes. *Physical Review B - Condensed Matter and Materials Physics* **62,** 5129 (2000).
23. Uryu, S. & Ando, T. Electronic intertube transfer in double-wall carbon nanotubes. *Physical Review B - Condensed Matter and Materials Physics* **72,** 1–10 (2005).
24. Tomio, Y., Suzuura, H. & Ando, T. Interwall screening and excitons in double-wall carbon nanotubes. *Physical Review B - Condensed Matter and Materials Physics* **85,** 085411 (2012).
25. Levshov, D. *et al.* Experimental evidence of a mechanical coupling between layers in an individual double-walled carbon nanotube. *Nano Letters* **11,** 4800–4804 (2011).
26. Zhao, S. *et al.* Rayleigh scattering studies on inter-layer interactions in structure-defined individual double-wall carbon nanotubes. *Nano Research* **7,** 1548–1555 (2014).
27. Hirschmann, T. C. *et al.* Role of intertube interactions in double-and triple-walled carbon nanotubes. *ACS Nano* **8,** 1330–1341 (2014).
28. Liu, K. *et al.* Van der Waals-coupled electronic states in incommensurate double-walled carbon nanotubes. *Nature Physics* **10,** 737–742 (2014).
29. Koshino, M., Moon, P. & Son, Y. W. Incommensurate double-walled carbon nanotubes as one-dimensional moiré crystals. *Physical Review B - Condensed Matter and Materials Physics* **91,** 035405 (2015).
30. Berciaud, S. *et al.* Excitons and high-order optical transitions in individual carbon nanotubes: A Rayleigh scattering spectroscopy study. *Physical Review B* **81,** 041414 (2010).
31. See Supplemental Material at [url] for experimental and theoretical results on the DWCNT structures and spectra, which includes Refs. [29,32-36].
32. Liu, K. *et al.* An atlas of carbon nanotube optical transitions. *Nature Nanotechnology* **7,** 325–329 (2012).
33. S. Choi, J. Deslippe, R. B. Capaz, S. G. Louie. An Explicit Formula for Optical Oscillator Strength of Excitons in Semiconducting Single-Walled Carbon Nanotubes: Family Behavior. *Nano Lett.* **13**, 54-58 (2013).
34. S. Uryu. Electronic states and quantum transport in double-wall carbon nanotubes. *Phys. Rev. B* **69**, 075402 (2004)
35. T. Ando. Theory of Electronic States and Transport in Carbon Nanotubes. *J. Phys. Soc. Jpn.* **74**, 777-817 (2005)
36. M. Koshino & N. N. T. Nam. Continuum model for relaxed twisted bilayer graphenes and moiré electron-phonon interaction. *arXiv:1909.10786* (2019)
37. Liu, Z. & Qin, L. C. A direct method to determine the chiral indices of carbon nanotubes. *Chemical Physics Letters* **408,** 75–79 (2005).
38. Liu, K. *et al.* Direct determination of atomic structure of large-indexed carbon nanotubes by electron diffraction: Application to double-walled nanotubes. *Journal of Physics D: Applied Physics* **42,** (2009).
39. Torrens, O. N., Zheng, M. & Kikkawa, J. M. Direct experimental evidence of exciton-phonon bound states in carbon nanotubes. *Physical Review Letters* **101**, 157401 (2008).
40. Berciaud, S. *et al.* Excitons and high-order optical transitions in individual carbon nanotubes: A Rayleigh scattering spectroscopy study. *Physical Review B* **81,** 041414 (2010).
41. Uryu, S. & Ando, T. Exciton absorption of perpendicularly polarized light in carbon nanotubes. *Physical Review B - Condensed Matter and Materials Physics* **74**, 155411 (2006)